

Domain-Invariant Proposals based on a Balanced Domain Classifier for Object Detection

Zhize Wu^a, Xiaofeng Wang^b, Tong Xu^c, Xuebin Yang^c, Le Zou^b, Lixiang Xu^b,
Thomas Weise^a

^a*Institute of Applied Optimization, School of Artificial Intelligence and Big Data, Hefei University, Hefei, 230601, China.*

^b*School of Artificial Intelligence and Big Data, Hefei University, Hefei, 230601, China.*

^c*School of Computer Science and Technology, University of Science and Technology of China, Hefei, 230026, China.*

Abstract

Object recognition from images means to automatically find object(s) of interest and to return their category and location information. Benefiting from research on deep learning, like convolutional neural networks (CNNs) and generative adversarial networks, the performance in this field has been improved significantly, especially when training and test data are drawn from similar distributions. However, mismatching distributions, i.e., domain shifts, lead to a significant performance drop. In this paper, we build domain-invariant detectors by learning domain classifiers via adversarial training. Based on the previous works that align image and instance level features, we mitigate the domain shift further by introducing a domain adaptation component at the region level within Faster R-CNN. We embed a domain classification network in the region proposal network (RPN) using adversarial learning. The RPN can now generate accurate region proposals in different domains by effectively aligning the features between them. To mitigate the unstable convergence during the adversarial learning, we introduce a balanced domain classifier as well as a network learning rate adjustment strategy. We conduct comprehensive experiments using four standard

*Corresponding author

Email addresses: wuzz@hfu.edu.cn (Zhize Wu), xfwang@hfu.edu.cn (Xiaofeng Wang), tongxu@ustc.edu.cn (Tong Xu), yangxb@mail.ustc.edu.cn (Xuebin Yang), zoule@hfu.edu.cn (Le Zou), lixiangxu@hfu.edu.cn (Lixiang Xu), tweise@hfu.edu.cn (Thomas Weise)

datasets. The results demonstrate the effectiveness and robustness of our object detection approach in domain shift scenarios.

Keywords: Object Detection, Domain Adaptation, Adversarial Learning, Domain Classifier, Region Proposal Network.

1. Introduction

Object detection is a fundamental problem in computer vision. It aims at automatically finding the category and location information of object(s) of interest in an image. With the research and development of deep convolutional neural networks (CNNs), object detection approaches with excellent performance have emerged. Breakthroughs have been achieved on standard benchmark datasets. For example, the average precision on the COCO dataset [1] has leaped from 35% in 2016 to 61% today [2].

Detection models are usually trained based on images with similar characteristics, i.e., on images from one domain. Training and test data are then drawn from identical distributions. However, in practice, the models may be applied to another domain where, for instance, the background, illumination, or the appearance of the objects are different [3]. The features computed from the new and different type of images then may not match well to those the object classifiers have been trained on – the so-called domain shift appears. The models then suffer from a steep performance decay [4]. Figure 1 shows an example of domain shift: The impact of changed weather conditions on the performance of object detection is very obvious and very negative.

Sufficiently much annotated data could mitigate the domain shift problem to some extent. Since there is no shortcut around manual labeling to obtain object annotation information, acquiring and annotating a large amount of data is time-consuming and labor-intensive. One approach to mitigate this problem is to perform style transfer [7] between a labeled and an unlabeled dataset. This method uses a Generative Adversarial Network (GAN) to produce data with the same style as the target domain. It therefore requires training a generative

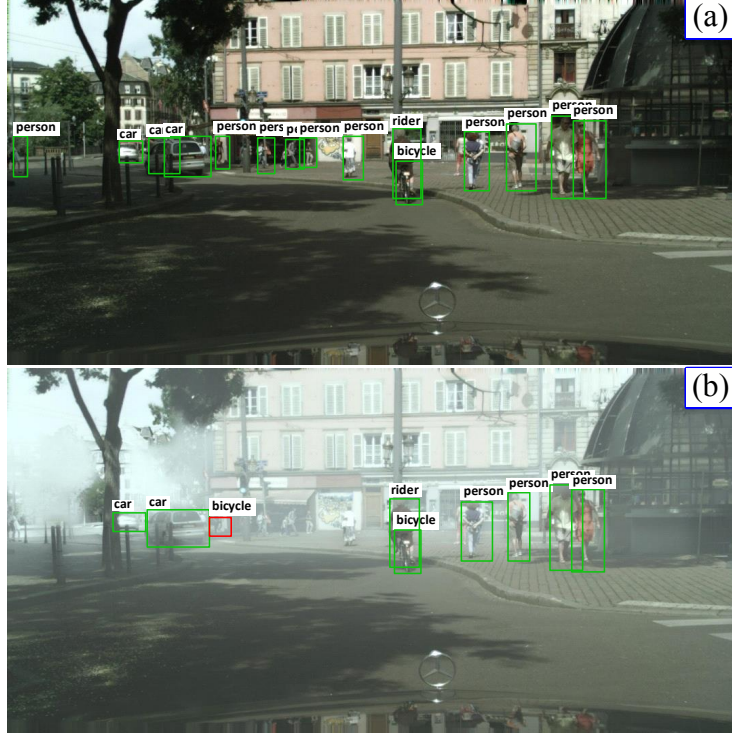


Figure 1: Performance decay from domain shift. (a) and (b) are the detection results on Cityscapes [5] and Foggy Cityscapes [6], respectively. Only Cityscapes was used for training.

and a discriminant network, which results in higher complexity. The quality of the image-style transformation also greatly affects the performance of the subsequent object detection.

Domain adaptive object detection (DAOD) [8] aims to provide a solution to the above problems. It extracts domain-independent features. The features of different domains are mapped to the same feature space to transfer semantic supervision information. Finding a good approach to measure the learned features in different domains and to examine whether they are consistent is the key to achieving this goal. The latest domain classifier based methods perform well in cross-domain object detection. They classify whether a data point is drawn from the target or source domain using domain discriminators. They also conduct adversarial training to encourage domain confusion [8].

Domain Adaptive (DA) Faster R-CNN [3], which we will refer to as DA-Faster, was the first domain classifier based work to tackle the cross-domain object detection problem. It applied the H-divergence to measure the difference between the data distribution of the target domain and source domain. In order to reduce the domain discrepancy, its authors designed domain adaptation components by embedding domain classifiers at image and instance level. In a more recent work, they observed that a big variance in object scales is challenging for cross-domain object detection [9]. Therefore, they further improve the DA-Faster model by explicitly incorporating the object scale into the adversarial training.

The Faster R-CNN [10], the basis of DA-Faster, achieved a major breakthrough in object detection by introducing the Region Proposal Network (RPN), which proposes regions that are likely to contain objects of interests. However, even in DA-Faster, it is difficult for the RPN to generate accurate region proposals in the target domain for cross-domain object detection. Previous studies rarely considered the RPN and instead mostly aligned features in the feature extraction network, the region-based classification, and the regression network.

We introduce the generation of domain-invariant region proposals into DA-Faster by developing a domain-invariant region proposal network (DIR). Here, the generator network is the convolution part of Faster R-CNN used to extract features. The discriminator network is an embedded domain classification network. Now, the RPN can generate accurate region proposals by aligning the features between different domains. We further design a double consistency regularization for eliminating the domain shift between domain classifiers at image, region, and instance level, and improve the generalization ability of the cross-domain object detection model.

We then encountered the problem that the learning abilities of the convolutional generator and the domain discriminator are imbalanced. As a result, the model training becomes unstable. The convolutional adversarial network is responsible for extracting features that contain as little domain shift as possible. This complicates the task of the domain classification network, which should

determine the right domain label based on the feature maps returned by the convolutional adversarial network. In the resulting adversarial game, it is easy for one of these networks to develop better abilities than the other. This then prevents the model from converging properly.

We propose a balanced domain classifier (BDC) where the network structure is adjusted to solve this problem. After studying the number of convolutional layers and the number and size of convolution kernels of the domain classification network, we design a network structure where the domain classification network matches the convolutional adversarial network in terms of learning ability. We additionally adjust the learning rate according to the gradient to improve the network weight updates.

We conduct comprehensive experiments using four standard datasets. Our results show the effectiveness and robustness of our method for object detection in multiple domain shift scenarios. Our main contributions are summarized as follows.

1. We propose the domain-invariant region proposal network DIR and incorporate a double consistency regularization method for eliminating the domain shift between domain classifiers at image, region, and instance level.
2. We propose the balanced domain classifier BDC to make up for the mismatch in learning ability between the convolutional generator network and the domain discriminator network.
3. We devise a learning rate adjustment strategy, which improves the convergence of the cross-domain object detection model.

The remainder of this paper is organized as follows. Section 2 provides an overview of the related work on DAOD methods. In Section 3, we introduce the preliminaries of our proposals, and in Sections 4 and 5, we present the DIR and BDC, respectively. In Section 6, we evaluate the algorithm performance. The conclusions and discussion are given in Section 7.

2. Related Work

We now provide an overview of works on object detection and domain adaptation. We refer the readers to [11] for a recent review of generic deep learning based object detection methods and to [8] for a recent review of domain adaptation based cross-domain object detection methods.

Object detection literature mainly focuses on the single-domain setting, where training and validation are performed on different samples from the same data distribution. Generic object detection methods can be categorized into two groups. The first one regards object detection as a regression or classification problem and adopts a unified framework to directly produce the categories and locations. Prominent members of this group are the YOLO family [12, 13], SSD [14], G-CNN [15], DSSD [16], and DSOD [17]. The second group of object detectors generates region proposals and then classifies each proposal into its object category. R-CNN [18], SPP-net [19], Fast R-CNN [20], Faster R-CNN [10], R-FCN [21], FPNs [22], and the Mask R-CNN [23] are popular such methods.

Domain adaptive object detection (DAOD) aims to generalize the models learned from a labeled source domain to another, unlabeled target domain. DOAD approaches are mainly based on the second group of object detection methods.

One idea is to reduce the domain shift by fine-tuning detection models with labeled or unlabeled target data [24, 25, 26, 27, 28, 29, 30, 31]: Khodabandeh *et al.* [24] tackled domain adaptation from the perspective of robust learning and formulate the problem as training with noisy labels. Cai *et al.* [25] simulated unsupervised domain adaptation as semi-supervised learning in their MTOR algorithm. MTOR remolds the Mean Teacher (MT) approach [26] under the backbone of Faster R-CNN by integrating the object relations into the measure of consistency cost between teacher and student modules. Recently, Deng *et al.* [27] revealed that there often exists a considerable model bias for the simple MT model in cross-domain scenarios. They mitigated this bias with several simple yet highly effective strategies in their UMT algo-

rithm. In [29], Mou *et al.* proposed a cycle semantic transfer network to align the instance-level and class-level distributions between the source domain and target domain and automatically label the hard samples. Xiong *et al.* [30] proposed global class prototypes to produce pseudo-labels for training the target model. With this, the source and target domains are also implicitly aligned.

Another approach is to apply adversarial training to encourage domain confusion between the source and target domains [3]. Here, domain discriminators are used to classify to which of the domains a data point belongs. The already-mentioned domain adaptive Faster R-CNN (DA-Faster) algorithm by Chen *et al.* [3] incorporates two domain adaptation components, one at image and one at instance level, into the Faster R-CNN model to minimize the H-divergence between two domains. Xie *et al.* [32] embedded multiple domain classification networks in the feature extraction network. To answer the questions “where to look” and “how to align,” Zhu *et al.* [33] followed the local nature of detection to reposition the focus of the adaptation process. In [34], Saito *et al.* proposed the unsupervised adaptation method SWDA for object detection that combines weak global alignment with strong local alignment, which are performed by a global and a local domain classifier, respectively. In the DD-MRL [35], an image-to-image translation via a GAN is used to generate images shifted from the source domain to the target domain for pixel-level adaptation. Chen *et al.* [36] proposed a Generative Attention Adversarial Classification Network (GAACN). The attention module in the process of adversarial learning allows the discriminator to distinguish the transferable regions among the source and target images.

More recently, Wang *et al.* [37] proposed an augmented feature alignment network (AFAN). The AFAN integrates adversarial feature alignment and an intermediate domain image generator into a single object detection framework. In the iFAN [38], an image-level alignment and a full instance-level alignment are introduced. Chen *et al.* [39] presented a framework called Hierarchical Transferability Calibration Network (HTCN) that harmonizes transferability and discriminability in the context of adversarial adaptation for adapting object de-

tectors. In [40], Liu *et al.* introduced a two-way alignment framework for unsupervised multisource domain adaptation.

We follow this line of research and focus on domain-invariant proposals and balanced domain classifiers for cross-domain object detection. We embed a domain classifier into the RPN phase of Faster R-CNN to obtain more precise instance-level feature representations. We observe that the imbalance between the convolution adversarial network and domain classification networks is challenging for the model training. We therefore design a balanced domain classifier to improve the model optimization.

3. Preliminaries

Adversarial-based DAOD methods utilize domain discriminators to classify whether a data point is drawn from the source or target domain. The adversarial training is used to encourage domain confusion. Our work adopts the main idea of DA-Faster [3], which contains two major parts: Image-Level Adaptation and Instance-Level Adaptation.

Image-Level Adaptation. A domain classifier is used to predict the domain label for each image patch, which reduces the image-level domain shift, such as image scale, style, etc. We define the loss function for the image-level adaptation as

$$\mathcal{L}_{image} = -\sum_{i,u,v} [D_i \log Base_i^{u,v} + (1-D_i) \log(1-Base_i^{u,v})] \quad (1)$$

where D_i denotes the real domain label of the i^{th} image: a value of 1 represents the target domain and 0 represents the source domain. $Base_i^{u,v}$ represents the domain prediction of the pixel at (u, v) on the feature map of the i^{th} image.

Instance-Level Adaptation. The instance-level adaptation loss is defined as

$$\mathcal{L}_{instance} = -\sum_{i,j} [D_i \log ins_{i,j} + (1-D_i) \log(1-ins_{i,j})] \quad (2)$$

where $ins_{i,j}$ represents the domain prediction of the j^{th} object instance in the i^{th} image.

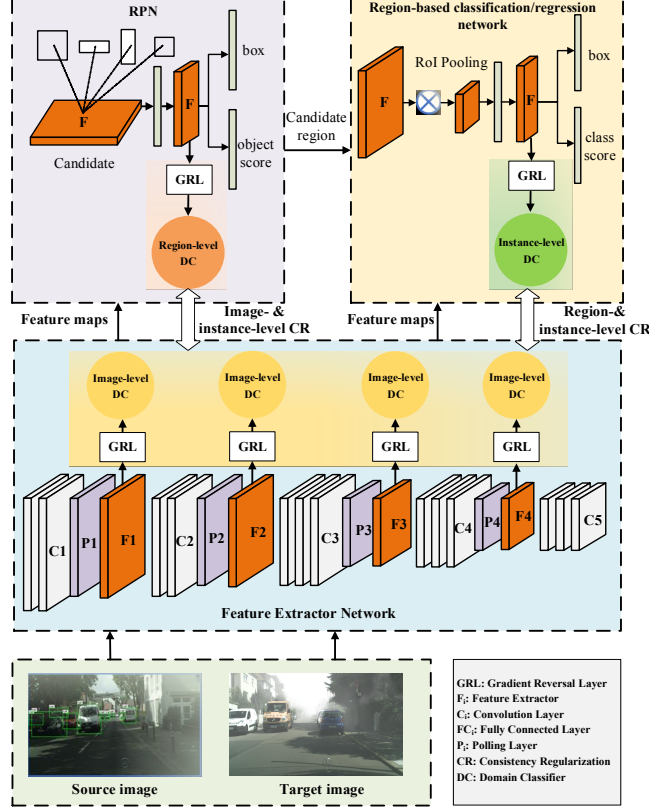


Figure 2: The architecture of DIR-FR. There are two components: (1) the Domain-Invariant RPN (DIR) using the region-based DC and (2) the Double-Consistency Regularization (DCR): Image-&Instance-level CR and RPN-&Instance-level CR. Additionally, we use multi-level image DCs to enhance the feature extractor.

Both adaptation components implement the adversarial training strategy by adding a Gradient Reverse Layer (GRL) [41] before the domain classifier. We refer the readers to [3] for more details about the network architecture and the implementation.

4. Domain-Invariant Region Proposal Network

We argue that making the RPN domain-invariant is essential to achieving effective cross-domain object detection with a Faster R-CNN based approach.

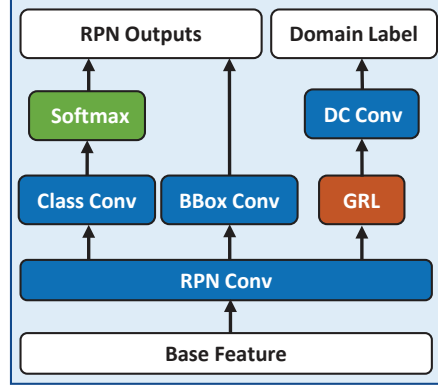


Figure 3: Architecture of the Domain-Invariant RPN

Hence, we design the Domain-Invariant Region Proposal Network (DIR) based on adversarial learning to obtain domain-invariant features, so that the RPN can also produce accurate proposals in the target domain. We introduce a Double-Consistency Regularization (DCR) method to eliminate the domain shift in the network between each domain adaptive module. In order to enable the feature extractor network to provide feature maps with less domain shift to the RPN, we borrow from the work of Xie *et al.* [32] and apply multiple image-level domain classifiers in the feature extractor network. We name our algorithm Faster R-CNN with Domain-Invariant RPN (DIR-FR). The framework of DIR-FR is shown in Figure 2. Next, we will introduce in detail the DIR module, the DCR, and the model architecture.

4.1. Domain-Invariant RPN (DIR)

We illustrate the DIR schematic in Figure 3. Differing from the original RPN in Faster R-CNN, our DIR is applicable to cross-domain object detection and can generate equally accurate bounding box proposals in different domains.

The DIR embeds a domain classifier after convolution on the input feature map, and trains the network using adversarial learning. In order to distinguish it from the image-level domain classifier in the feature extractor network and the instance-level domain classifier in the region-based classification and regres-

sion network, we call the domain classifier in the RPN the region-level domain classifier.

When it classifies the examples into target or source domains, the classification loss will pass a GRL before backpropagation to the RPN convolutional layer. The region-level domain classifier is responsible for predicting the domain label as accurately as possible on the feature map extracted by the RPN convolutional layer. After the gradient backpropagation, the updated network parameters will enable the region-level domain classifier to extract more features for assigning the right domain labels when predicting domain labels the next time. However, when the gradient passes through the GRL and then flows through the RPN convolutional layer, the extracted features of the RPN convolutional layer will reduce the information that can distinguish domain labels as much as possible. In this adversarial training manner, the RPN convolutional layer can learn to extract domain-invariant features that can deceive the region-level domain classifier. With this, the DIR can generate effective bounding box proposals for the target domain with the supervised annotations from the source domain.

A two-class standard cross-entropy function is used to calculate the domain prediction loss:

$$\mathcal{L}_{region} = -\sum_{i,j} [D_i \log Region_i^{u,v} + (1-D_i) \log(1-R_i^{u,v})] \quad (3)$$

where $Region^{u,v}$ denotes the output of the RPN domain classifier at (u, v) of the RPN feature map and D_i denotes the domain label of the i^{th} image.

4.2. Double-Consistency Regularization (DCR)

In order to further enhance the robustness of the cross-domain detector, we propose the Double Consistency Regularization (DCR) for eliminating the domain shift between the domain classifiers at all levels.

In DIR-FR, the data disturbance mainly comes from the domain classifier that uses adversarial learning during training. There are three domain classifiers, namely the one at image-level in the feature extractor network, the one

at region-level in the RPN, and the one at instance-level in the region-based classification and regression network. During the gradient backpropagation, this is prone to produce gradient counteraction between domain classifiers. For example, the prediction results may not be consistent when the instance- and the image-level domain classifiers predict the domain label of a specific class of image. The gradients of the two classifiers will be counteracting, so that there is not enough effective gradient information to learn domain-invariant features in the feature extractor network. As a result, the cross-domain detector cannot accurately detect the object in this class of images.

In order to mitigate the counteraction, we adopt a consistency regularization to effectively propagate the gradients obtained by each domain classifier. In particular, the regularization forces the same predictions of two domain classifiers and guides each module of the cross-domain object detection model to learn domain-invariant features. Single consistency regularization can only ensure that the predictions of two domain classifiers are the same, but our DIR-FR has three domain classification networks. Therefore, we propose a double consistency regularization method, i.e, the DCR. In the DCR, the consistency of the predictions of the classifiers include the consistency regularization of the image- and instance-level as well as of the region- and instance-level domain classification networks.

The two consistency regularizations are defined in Equations 4 and 5 below.

$$\mathcal{L}_{img\&ins_CR} = - \sum_{i,j} \left\| \frac{1}{|I|} \sum_{u,v} Base_i^{u,v} - Ins_{i,j} \right\|_2 \quad (4)$$

$$\mathcal{L}_{reg\&ins_CR} = - \sum_{i,j} \left\| \frac{1}{I} \sum_{u,v} Region_i^{u,v} - Ins_{i,j} \right\|_2 \quad (5)$$

Here, $|I|$ represents the number of features computed by the feature extractor network from the current image to be detected and $\|\cdot\|_2$ is the Euclidean norm. We add both consistency regularization terms and obtain the loss function of the DCR as Equation 6:

$$\mathcal{L}_{double_CR} = \mathcal{L}_{img\&ins_CR} + \mathcal{L}_{reg\&ins_CR} \quad (6)$$

4.3. Overall Objective for DIR-FR

DIR-FR is based on the Domain Adaptive Faster R-CNN discussed in Section 3. Its overall loss function is:

$$\mathcal{L} = \mathcal{L}_{det} + \lambda(\mathcal{L}_{image} + \mathcal{L}_{instance} + \mathcal{L}_{region} + \mathcal{L}_{double_CR}) \quad (7)$$

where \mathcal{L}_{det} is the object detection loss generated by the Faster R-CNN. λ controls the trade-off between the detection loss and the domain adaptive components. In our experiments, we set $\lambda = 0.1$.

5. Balanced Classification Network

As shown in Figure 2, we embed three domain classification networks into the DIR-FR framework and adopt a GRL based adversarial learning mechanism to train the cross-domain detector. How to keep a balanced adversarial game state between the domain classification network and the convolution network is the key to the detector training. Inspired by the training idea of GANs [42], we propose the balanced classification network construction method by analyzing the similarities and differences between the domain classifier and a GAN, as well as a learning rate adjustment strategy to promote a more stable model convergence. Combined with DIR, we build a new and improved cross-domain object detection model, namely balanced domain DIR (BD-DIR). Next, we discuss the differences and connections between domain classifiers and GANs.

5.1. Similarities and Differences between DC and GAN

Similarities. In the cross-domain object detection model embedded in the domain classifier, the model training in the way of adversarial learning is similar to the idea of GANs. The structure of the two models is also similar, as shown in Figure 4. The DC-based cross-domain detector expects that the convolution adversarial network can align the image features of the source domain and the target domain. Then, the detector can achieve equal performance in the target domain. This leads to the same design principles as in GANs: Both methods

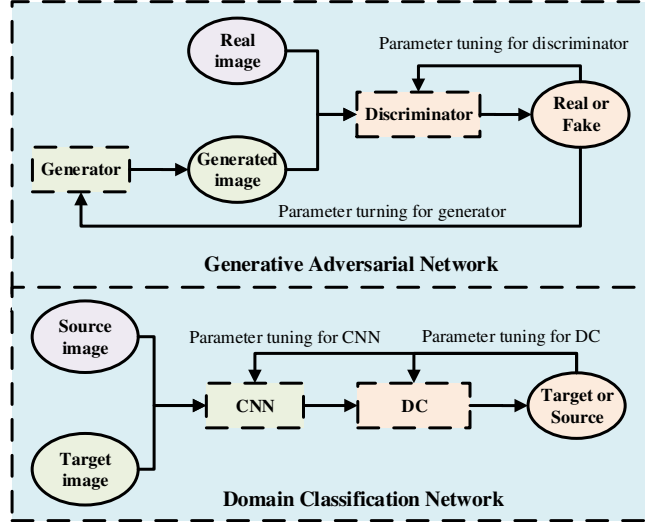


Figure 4: Structures of GANs and Domain Classifiers

build a pair of networks that form an opposite relationship in learning tasks. Both improve the ability of model learning through the competition between the two networks.

Differences. However, there is a big difference in the network training stage. Since the direction of the optimization objective function of the generator and the discriminator in GANs is exactly opposite, the two networks are trained separately in an iterative and alternating manner. In each step, the parameters of one of the networks are fixed and those of the other are trained. During the training process, the generator and the discriminator can be maintained in a balanced and adversarial state through manual intervention. The whole model can converge stably.

For the cross-domain object detection model embedded in the domain classification network, the GRL is generally used to make the convolutional adversarial network and the domain classification network obey the same optimization goals. Both exist to improve the accuracy of the domain classification network in predicting the domain label of the image. Therefore, the cross-domain detector and the prediction result of the domain classifier can be optimized at the

same time with end-to-end training. However, the competition between the convolutional adversarial network and the domain classification network can easily become unbalanced during this process. This can lead to instability, oscillation, and difficulties to converge to the equilibrium point during the training of the models.

5.2. Designing the Balanced Domain Classification Network

End-to-end training can be regarded as a modification of the alternate iterative training, but this modification strictly requires the convolutional adversarial network and the domain classification network to maintain the same number of training steps. In order to make the cross-domain object detection model converge steadily, the convolutional adversarial network and the domain classification network need to achieve a balanced learning ability. We therefore propose the idea of a balanced domain classification network. In the cross-domain object detection model based on DA-Faster, the convolutional adversarial network is the feature extractor network part. Therefore, we design a domain classification network that balances the learning ability of the convolutional adversarial network.

Chen *et al.* [3] were the first to apply a domain classifier to the cross-domain object detector. Subsequent works mainly followed this design: The image-level and region-level domain classification networks use two convolutional layers to extract features and then classify the features. Both convolutional layers are composed of 512 convolution kernels with a size of 1×1 . The instance-level domain classification network is composed of a fully connected layer, which classifies the region of interest features generated by ROI pooling. The number of input features of the fully connected layer is 4096, and the number of output categories is 2.

The design of the instance-level domain classification network is completely determined by the number of input features and the number of output categories. We do not create a special design for the instance-level domain classification network. That is, the domain classification networks we are concerned with are

image-level and region-level domain classification networks.

In addition to the number of convolution kernels, their size and the number of layers of the domain classification network are far smaller compared to the convolutional adversarial network. This also leads to a weaker ability of the domain classification network to discriminate domain labels when training cross-domain detection models. The convolutional adversarial network can easily deceive the domain classification network after a few iterations of training. At this time, the prediction result of the domain classification network is similar to a random value and cannot provide an effective optimization gradient for the convolutional adversarial network. On the other hand, if the domain classification network has strong learning ability, it can accurately predict the domain label of the image every time, which will cause the phenomenon of gradient disappearance.

Algorithm 1: Iterative control variable method

Input:

- (1) Number of convolutional layer parameters n ;
- (2) Convolutional layer parameters $p_i, i \in 0 \dots n - 1$;
- (3) Threshold δ .

Output: Convolutional layer parameters p_i .

```

1 Initialize  $p_i, i \leftarrow 0$ , and current accuracy  $acc_{now} \leftarrow 1$ ;
2 do
3   Fix parameter values other than  $p_i$  and optimize  $p_i$ ;
4    $acc_{pre} \leftarrow acc_{now}$ ;
5   Calculate the current accuracy of the cross-domain detection
      model  $acc_{now}$ ;
6    $i = (i + 1) \bmod n$ ;
7 while  $|acc_{now} - acc_{pre}| > \delta$ ;
```

In order to enable the domain classification network and the convolutional adversarial network to maintain a balanced confrontation game state during

training, we propose the concept of a balanced domain classification network. The number of convolutional layers, the number and size of convolution kernels, and the step size jointly control the receptive field and feature extraction capabilities of the domain classification network. We can therefore use these parameters to control the equalization of the learning ability of the domain classification network and the convolution adversarial network. Then, the domain classification network is a balanced domain classification network.

In order to obtain such a balanced domain classification network, it is not advisable to blindly search for the right parameters of the convolutional layer, as this is too time-consuming due to the huge search space. The receptive field and feature extraction capabilities of the domain classification network increase with the number of convolutional layers, the number of convolution kernels, and the size of the convolution kernels. In other words, increasing the values of these three parameters has a similar impact on the learning ability of the domain classification network. We propose an iterative control variable method to simplify searching parameters for a balanced domain classification network. Only one parameter is variable during each search, and the rest are fixed values. We iteratively repeat the above steps until the network reaches a better solution, as shown in Algorithm 1.

5.3. Learning Rate Adjustment

The learning rate is mainly used to control the strength of adjusting parameters of the detection model. When the learning rate is large, the cross-domain object detection model adjusts the parameters in larger steps. The detection model can converge faster, but this can also cause the model to miss a better equilibrium point. When the learning rate is small, although the network converges to a better equilibrium point with high probability, it often needs more training rounds because of the smaller step size in parameter adjustment. This results in an unnecessary waste of computing resources. An appropriate learning rate adjustment strategy can improve the training efficiency of cross-domain object detection models.

In order to enable the cross-domain object detection model to converge to a better solution, we design a learning rate adjustment strategy that is suitable for training based on adversarial learning methods. We could follow [32] and set the learning rate α in our DIR-FR initially to, say, $2e^{-3}$ and then multiply it by, for instance, 0.1 after six iterations. This would lead to fast convergence in the early stage. The learning rate reduction later on would be helpful for the detection model to converge to the equilibrium point. However, this adaptation method would not make use of the information provided by the prediction error of the cross-domain object detection model. When this prediction error is large, then the model has a large learning space. Its parameters then can be adjusted with a large learning rate to speed up the convergence. When the error is small, the model has converged closely to the equilibrium point. At this time, it only needs a small learning rate to fine tune the parameters. Therefore, we design a learning rate adjustment strategy using the prediction error of the cross-domain detection model. The specific adjustment is shown in Equation 8.

$$\alpha = \begin{cases} \alpha_{up} & \text{if } t_{up} \leq loss \\ \alpha_{low} & \text{else if } loss \leq t_{low} \\ \alpha_{low} + \frac{loss - t_{low}}{t_{up} - t_{low}}(\alpha_{up} - \alpha_{low}) & \text{otherwise} \end{cases} \quad (8)$$

where α is the learning rate of the training round about to start, $loss$ is the prediction error of the current iteration, and α_{up} and α_{low} are the maximum and minimum learning rates, respectively. t_{up} and t_{low} are the upper and lower thresholds of the prediction loss of the cross-domain object detection model. They are used for preventing α from exceeding $[\alpha_{low}, \alpha_{up}]$. We here set α_{up} and α_{low} to $2e^{-3}$ and $2e^{-5}$ and t_{up} and t_{low} to 12 and 1, respectively.

6. Experiments and Results

We now evaluate our proposed methods with comprehensive experiments on four public datasets, namely KITTI [43], Cityscapes [5], SIM 10k [44], and Foggy Cityscapes [6]. Following [3], we first perform experiments on three different domain shift scenarios, i.e., Cityscapes \rightarrow Foggy Cityscapes, SIM 10k

\rightarrow Cityscapes, and Cityscapes \rightarrow KITTI. These shifts correspond to adverse weather adaptation, synthetic data adaptation, and cross camera adaptation, respectively. Then, we carry out ablation experiments to verify the utility of DIR-FR and BDC. Finally, we perform a visual analysis.

6.1. Experimental Setup and Evaluation Criteria

We follow the unsupervised domain adaptation protocol in the experiments. The training data has two parts. For the target domain training data, only unlabelled images are provided. The training data for the source domain has the annotations (bounding boxes and object categories).

We design the BDC only once and use it in all experiments. We set the threshold δ in Algorithm 1 to 0.005. We construct the BDC for the weather adaptation task and use it in all experiments, because it has the most categories and the categories in the other experiments are only subsets of thereof. During the training, the source domain data loss is composed of the object detection loss and the adaptive component loss. The target domain data loss is only composed of the adaptive component loss.

The adaptive components do not participate in the inference calculation, so the inference speed of our DIR-FR is the same as for Faster R-CNN.

We use VGG-16 [45] as the model backbone and pretrain it on ImageNet [46]. We employ the SGD optimizer and set the weight decay to $5e^{-4}$ and the momentum to 0.9. Before introducing the BDC into DIR-FR, the learning rate is initially $2e^{-3}$ and will reduce to $2e^{-4}$ after six epochs.

The images from the four datasets have different sizes. We therefore scale the images such that their shorter sides measure 600 pixels.

We train the network for ten epochs on the source and target domain training data. The adapted model is tested on 500 images from the target domain. As environment for all experiments, we use Ubuntu 16.04 on an Intel Core i7-7700 processor with 32 GB RAM and an Nvidia GTX 1080Ti graphics card. We compute three performance indexes: the average precision (AP), the mean average precision (mAP), and the mean intersection over union (mIOU). The

Table 1: Results on adaptation from Cityscapes to Foggy Cityscapes

Method	Person	Rider	Car	Truck	Bus	Train	Motorcycle	Bicycle	mAP
Faster R-CNN [10]	24.5	32.7	35.4	12.7	26.7	9.2	9.9	30.0	22.6
DA-Faster [3]	31.9	41.6	46.4	20.1	32.5	17.5	23.1	34.6	30.9
SWDA [34]	29.9	42.3	43.5	24.5	36.2	32.6	30.0	35.3	34.3
SCDA [33]	33.5	38.0	48.5	26.5	39.0	23.3	28.0	33.6	33.8
DD-MRL [35]	30.8	40.5	44.3	27.2	38.4	34.5	28.4	32.2	34.6
MTOR [25]	30.6	41.4	44.0	21.9	38.6	40.6	28.3	35.6	35.1
MDA [32]	33.2	44.2	44.8	28.2	41.8	28.7	30.5	36.5	36.0
iFAN [38]	32.6	40.0	48.5	27.9	45.5	31.7	22.8	33.0	35.3
HTCN [39]	33.2	47.5	47.9	31.6	47.4	40.9	32.3	37.1	39.8
UMT [27]	33.0	46.7	48.6	34.1	56.5	46.8	30.4	37.3	41.7
DIR (ours)	36.9	45.8	49.4	28.2	44.6	34.9	35.1	38.9	39.2
DB-DIR (ours)	38.2	48.4	52.9	29.8	51.0	43.3	37.1	41.9	42.8

AP is used to measure the average accuracy of our cross-domain object detection models. The mAP represents the average accuracy of the models for multiple categories, which is the average of the AP values for each detection category. Following [3], we also use the mIOU in our visual analysis in Section 6.4.

6.2. Experimental Results

Adverse Weather Adaptation. In this experiment, we adapt detection models from normal to foggy weather. Weather is an important cause of domain shift. It is critical that a detector can operate reliably under different weather conditions. We therefore use the Cityscapes and Foggy Cityscapes datasets as source and target domain, respectively. The Foggy Cityscapes dataset is rendered from the original clear-weather images by simulating fog on real scenes. There are 2975 images in the training set and 500 images in the validation set. Our reported results on all categories are on the validation set.

Besides the Faster R-CNN baseline [10], we further include DA-Faster [3], SWDA [34], SCDA [33], MTOR [25], MDA [32], iFAN [38], DD-MRL [35], HTCN [39], and UMT [27] for comparison, all of which have been discussed in Section 2. The experimental results are shown in Table 1.

Object detection in foggy scene images is extremely challenging due to low

Table 2: Results of the adaptation from SIM 10k to Cityscapes in terms of the AP

Method	AP on <i>car</i>
Faster R-CNN [10]	34.2
DA-Faster [3]	39.2
SWDA [34]	40.1
SWDA ($\gamma = 3$) [34]	42.3
SCDA [33]	43.0
MDA [32]	42.0
iFAN [38]	46.9
HTCN [39]	42.5
UMT [27]	43.1
DIR (ours)	45.5
DB-DIR (ours)	45.3

visibility. From Table 1, we find that our DB-DIR achieves the highest mAP and performs best in the five categories *person*, *rider*, *car*, *motorcycle*, and *bicycle*. The current best result on this dataset is 41.7% from the recent work UMT [27]. However, our DIR model already approaches UMT with a mAP of 38.9%. This validates the effectiveness of the region-level adaptation for improving the DA-Faster model for cross-domain object detection. By building the balanced domain classification network, our final DB-DIR model surpasses the UMT and reaches an mAP of 42.8%.

Synthetic Data Adaptation. In this experiment, we aim to adapt models trained on data from video games to the real world. We utilized the SIM 10k dataset as the synthetic source domain and the Cityscapes dataset as the target domain. There are 10000 images and 58701 bounding boxes of cars in the SIM 10k dataset. All the images are used for training. We report the average precision of the cars on the Cityscapes validation set, since *car* is the only category annotated in SIM 10k. The AP values for detecting cars for different approaches are reported in Table 2.

Both DIR and DB-DIR can eliminate the domain shift between synthetic data and real scene data. Compared with the baseline Faster R-CNN, DIR has improved the AP by 11.3%. There is only a slight gap of 1.4% to the best state-of-the-art method, iFAN.

The balanced domain classifier allows for a shorter training time. Only 9 epochs were needed for training DB-DIR – one less than for DIR. Yet, DB-DIR achieves an AP of 45.3%. We argue that the (very mild) performance degradation of DB-DIR in comparison to DIR is mainly caused by the decrease in the difficulty of the detection task. In the weather adaptation task, eight object categories need to be detected. Therefore, the domain classification network needed to have a high learning ability to predict domain labels. The use of a domain classification network of the same design on the synthetic data domain adaptation – which only contains one object category and has lower detection difficulty – results in a decrease in the accuracy of the detection model. This also shows that in the cross-domain object detection model, the domain classification network not only needs to be in a balanced state with the convolutional adversarial network in terms of learning ability, but also needs to have an adaptive learning ability for the detection task.

Cross Camera Adaptation. In this experiment, we adapt models for images under different camera setups. We utilized the Cityscapes dataset as the source domain and KITTI dataset as the target domain. The KITTI dataset consists of 7481 images, which have an original resolution of 1250×375 pixels. The KITTI dataset is used in both adaptation and evaluation. The experimental results are shown in Table 3.

From the experimental results, we find that our DB-DIR achieves the new state-of-the-art AP of 44.1% and DIR reaches 44.0%, which again demonstrates the effectiveness of our proposed approach. Compared with the Faster R-CNN baseline, DA-Faster and MDA, DB-DIR achieves a performance improvement of 9.4%, 7.8%, and 3.4%. We find that the MDA model is very suited for the detection of trains, while the performances of other categories are greatly improved by our methods.

Table 3: Results on adaptation from Cityscapes to KITTI

Method	Person	Rider	Car	Truck	Train	mAP
Faster R-CNN [10]	43.3	28.6	73.9	13.6	14.0	34.7
DA-Faster [3]	40.7	24.8	73.5	24.3	18.2	36.3
MDA [32]	53.0	24.5	72.2	28.7	25.3	40.7
DIR (ours)	58.5	37.2	75.4	30.6	18.5	44.0
DB-DIR (ours)	54.4	37.5	73.1	39.0	15.0	44.1

Table 4: Ablations of DIR on adaptation from Cityscapes to Foggy Cityscapes

Method	RDC	DCR	MIDC	Person	Rider	Car	Truck	Bus	Train	Motorcycle	Bicycle	mAP
Faster R-CNN				24.5	32.7	35.4	12.7	26.7	9.2	9.9	30.0	22.6
DA-Faster				31.9	41.6	46.4	20.1	32.5	17.5	23.1	34.6	30.9
MDA			✓	33.2	44.2	44.8	28.2	41.8	28.7	30.5	36.5	36.0
	✓			32.3	41.8	47.0	22.6	38.4	24.1	28.6	36.3	33.9
	✓	✓		33.4	45.9	48.8	28.3	38.3	15.7	32.4	38.9	35.2
DIR			✓	34.1	47.0	49.9	25.7	43.4	31.0	33.8	39.6	38.1
	✓	✓	✓	36.9	45.8	49.4	28.2	44.6	34.9	35.1	38.9	39.2

Similar to the results of synthetic data adaptation, DB-DIR has a slight advantage (0.1%) over DIR. It again takes 9 epochs for DB-DIR to converge, which is faster than DIR (10 epochs). Compared with Foggy Cityscapes that contains eight object classes, the difficulty of KITTI with its five classes is lower.

6.3. Ablation Study

We now investigate the ablations of the region-level domain classifier (RDC), the DCR, and the multiple image-level domain classifier (MIDC) for the DIR model. We further analyze the influence of network structure and learning rate on the DB-DIR.

6.3.1. Ablations of RDC, DCR, and MIDC for DIR

We conduct ablation experiments in both the adverse weather domain adaptation and the synthetic data adaptation. All adaptive components are added on the basis of DA-Faster. The experimental results are shown in Tables 4 and 5.

Table 5: Ablations of DIR on adaptation from SIM 10k to Cityscapes

Method	RDC	DCR	MIDC	Car
Faster R-CNN				34.2
DA-Faster				39.2
MDA			✓	42.0
DIR	✓			40.7
	✓	✓		41.6
	✓		✓	45.1
	✓	✓	✓	45.5

From the results of the adaptive ablation experiment in the severe weather domain in Table 4, we find that when only the RDC is used, the mAP increases from 30.9% to 33.9% compared with DA-Faster. Adding the DCR can further increase the mAP to 35.2%. When both the RDC and the DCR components are applied to the cross-domain object detection model, the detection accuracy of most categories is close to or surpasses the state-of-the-art methods. If the MIDC proposed by Xie *et al.* [32] is further applied, the model can obtain an improvement of 4.0%. At this time, the detection accuracy of the model is much higher than the other methods. It is 3.2 percentage points better than the previous best-performing MDA method.

The results of the ablation experiment for the synthetic data adaptation are shown in Table 5. When combining all the adaptive components, the cross-domain object detection model can increase the detection accuracy of Faster R-CNN by 11.3%, from 34.2% to 45.5%. When we further embed the RDC and DCR domain adaptive components into the DA-Faster model, the accuracy increases by 2.4%, from 39.2% to 41.6%. When the RDC and the DCR are applied on the previous best performing MDA model, they increase the detection accuracy from 42.0% to 45.5%, i.e., by 3.5%.

From the results of the above experiments, we can conclude that the region-level adaptation and double consistency regularization in DIR can eliminate the

Table 6: Results of different kernel sizes on adaptation from Cityscapes to Foggy Cityscapes

Method	Person	Rider	Car	Truck	Bus	Train	Motorcycle	Bicycle	mAP
K1_512_C2	36.9	45.8	49.4	28.2	44.6	34.9	35.1	38.9	39.2
K3_512_C2	37.8	49.2	52.0	28.8	47.3	29.4	34.8	40.2	40.0
K5_512_C2	39.1	49.9	52.8	30.3	51.2	33.1	37.6	40.3	41.8
K7_512_C2	38.8	49.1	52.8	30.8	50.8	34.1	39.5	39.5	41.9

Table 7: Results of different numbers of kernels on adaptation from Cityscapes to Foggy Cityscapes

Method	Person	Rider	Car	Truck	Bus	Train	Motorcycle	Bicycle	mAP
K3_512_C2	37.8	49.2	52.0	28.8	47.3	29.4	34.8	40.2	40.0
K3_1024_C2	38.2	48.0	52.4	30.7	46.2	35.4	35.1	40.9	40.9
K3_2048_C2	38.5	50.1	52.4	31.1	48.4	27.7	33.9	41.1	40.4

domain shifts between the source domain dataset and the target domain dataset, thereby improving the performance of the cross-domain object detection model.

6.3.2. Ablations of Network Structure and Learning Rate for DB-DIR

We now use the diverse weather domain adaptive experiment to construct the balanced domain classification network. Tables 6, 7, and 8, respectively show the effects of the size K of the convolution kernel, the number C of convolution kernels, and the number of convolutional layers (noted between K and C). For example, “K3_1024_C2” means that the domain classification network has 2 convolutional layers and each layer has 1024 3×3 convolution kernels.

Table 8: Results of different convolutional layers on adaptation from Cityscapes to Foggy Cityscapes

Method	Person	Rider	Car	Truck	Bus	Train	Motorcycle	Bicycle	mAP
K3_512_C2	37.8	49.2	52.0	28.8	47.3	29.4	34.8	40.2	40.0
K3_512_C3	38.1	48.8	52.8	28.9	48.2	45.3	36.7	42.4	42.6
K3_512_C4	38.3	46.5	52.7	28.0	51.1	28.3	36.1	41.8	40.3

Table 6 shows that, as the size of the convolution kernel increases, the accuracy of the detection model gradually improves. When the convolution kernel is expanded from 1×1 to 3×3 and then to 5×5 , the detection accuracy improves the most, increasing by 0.8% and 1.8%, respectively. When the convolution kernel is further expanded to 7×7 , the detection accuracy improves only slightly (by 0.1%). This shows that the imbalance between the convolution adversarial network and domain classification networks leads to a degradation of the cross-domain object detector.

Comparing Tables 7 and 6, we find that the number of convolution kernels in each convolutional layer of the domain classification network has less impact on the detection accuracy of the detection model than the size of the convolution kernel. The overall detection accuracy does not change by more than 0.9%. When the number of convolution kernels grows, the detection accuracy also does not always increase as well. When the number of convolution kernels is doubled from 512 to 1024, the detection accuracy rises by 0.9%, but when the number of convolution kernels is further increased to 2048, the detection accuracy drops by 0.5% instead.

From Table 8, we find that, as the number of convolutional layers in the domain classification network increases, the detection accuracy first improves and then declines again. When moving from 2 to 3 layers, the detection accuracy increases by 2.6%. Further increasing the number of layers to 4, however, causes a decrease of 2.3% in detection accuracy, which then is close to the result of using 2 convolutional layers. This shows that when the learning ability of the domain classification network is too strong and exceeds the learning ability of the convolutional adversarial network, the accuracy of the detection model will degrade.

Table 9 shows the results of ablation experiments based on the cross-domain object detection model of DB-DIR, where LRD refers to the learning rate adjustment strategy. It can be seen that DB-DIR improves the mAP by 3.4% (from 39.2% to 42.6%) on the basis of DIR, and the learning rate strategy LRD further improves the detection accuracy to 42.9%.

Table 9: Ablations for DB-DIR on adaptation from Cityscapes to Foggy Cityscapes

Method	Person	Rider	Car	Truck	Bus	Train	Motorecycle	Bicycle	mAP
K1_512.C2 (DIR)	36.9	45.8	49.4	28.2	44.6	34.9	35.1	38.9	39.2
K3_512.C2	37.8	49.2	52.0	28.8	47.3	29.4	34.8	40.2	40.0
K3_512.C3	38.1	48.8	52.8	28.9	48.2	45.3	36.7	42.4	42.6
K3_512.C2+LRD (DB-DIR)	38.2	48.8	52.9	29.8	51.0	43.3	37.1	41.9	42.9

The results of the above experiments show that the domain balanced classification network can help the model to converge to a better solution. At the same time, the results also verify the importance of maintaining a balanced game state between the domain classification network and the convolutional adversarial network when training the cross-domain object detection model based on the domain classification network. In addition, the learning rate adjustment strategy we proposed can further improve the accuracy of the cross-domain object detection model, so that DB-DIR can achieve the best detection results.

6.4. Visualization Analysis

We now verify whether the domain-invariant region proposal network and the double consistency regularization method can effectively reduce the inaccurate target positioning, missed detections, and serious misdetections of the cross-domain target detection model. Following Chen *et al.* [3], we quantitatively analyze the regions of interest generated by the region suggestion network. We divide them into three categories, namely, accurately positioned, inaccurately positioned, and background. A region of interest is accurately positioned if it corresponds to a real target, and the IOU between the region of interest and the real target is greater than 0.5. An inaccurately positioned region of interest has an IOU with the real target greater than 0.3 but less than or equal to 0.5. The regions of interest whose IOU with a real target is not greater than 0.3 are considered as background.

Figure 5 shows the experimental results of the severe weather domain adaptation experiment. *Ours* ($R\&D$) refers to the use of domain-invariant region proposal network and double-consistency regularization based on DA-Faster.

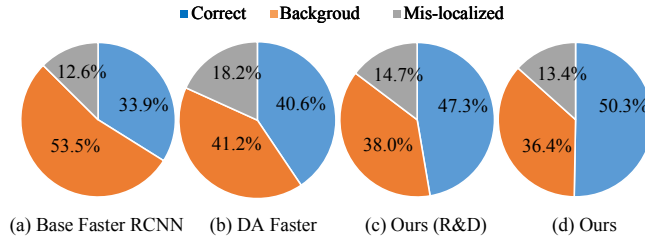


Figure 5: Error analysis of the proposals on experiments

Ours is the cross-domain target detection model DIR proposed in this article. Compared with *Ours (R&D)*, DIR embeds a multi-layer image-level domain classification network in the feature extractor network. Figure 5 shows that the two methods we proposed can effectively increase the proportion of accurately located regions of interest, and the proportion of inaccurately located regions of interest and background regions are significantly less than that of previous methods.

In the severe weather domain adaptation experiment, Faster R-CNN achieves an mIOU of 69.46% and DA-Faster 70.67%. The domain-invariant region proposal network and the double-layer consistency regularization method proposed in this article can improve the mIOU by 1.25%, from 70.67% to 71.92%. The above experimental results all prove that our method can effectively reduce inaccurate target positioning, missed detections, and serious misdetections in the cross-domain target detection model.

Figure 6 illustrates the example of detection results of the transfers from Cityscapes to Foggy Cityscapes, from Sim10K to Cityscapes, and from Cityscapes to KITTI, respectively. From top to bottom, there are examples of the detection results of the cross-domain object detection models DA-Faster, DIR, and DB-DIR. The green boxes in the figure are the result of correct detection. The red boxes mark misdetections and missed detections. Both DIR and DB-DIR consistently outperform the DA-Faster model in different tasks. DB-DIR performs the best. For example, on Foggy Cityscapes, DB-DIR is capable of detecting even the obscured instances with accurate bounding box predictions.

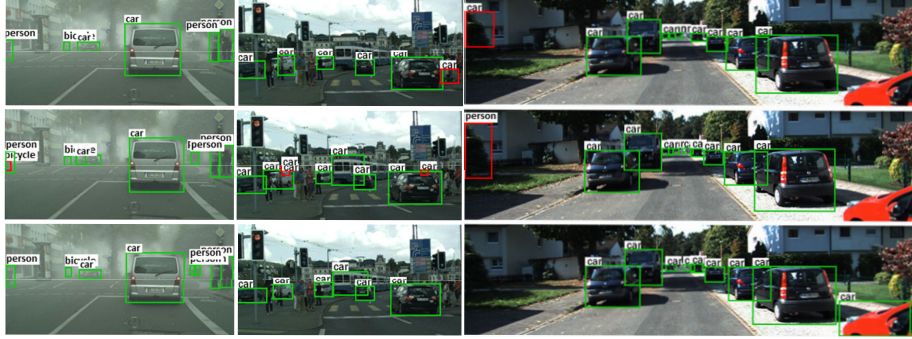


Figure 6: Illustration of the detection results on the target domain: First column: Cityscapes \rightarrow Foggy Cityscapes; Second column: SIM 10k \rightarrow Cityscapes; Third column: Cityscapes \rightarrow KITTI.

7. Conclusions

Object detection methods today have reached a high performance in identifying and localizing object instances of certain categories in an input image. However, if a domain shift occurs, i.e., if objects need to be detected from images that differ significantly those used during training, the accuracy drops sharply. A change in weather conditions, for example, can represent such a domain shift. It is necessary to develop algorithms that maintain good detection performance in a new domain without the need of collecting additional ground-truth annotations.

In this paper, we have introduced the Domain-Invariant RPN (DIR) based domain adaptive model, an effective approach for cross-domain object detection. DIR embeds a region-level domain classifier in the RPN and learns domain-invariant features via adversarial training, which eliminates the domain shift in the RPN. By enforcing the consistency of the prediction results of each domain classifier, the double consistency regularization aligns the features between the domain adaptation components. In addition, we design a domain classification network structure to obtain a balanced domain classifier (DB-DIR), which has a learning ability equivalent to a convolutional adversarial network. In order to improve the convergence of the cross-domain object detection model, we also

proposed a suitable learning rate adjustment strategy. This strategy uses the prediction loss to adjust the learning rate, which helps the cross-domain object detection model converge to a better solution.

Extensive experiments demonstrate that our approach surpasses the state-of-the-art performance for adapting object detectors on several benchmark datasets. When adapting from Cityscapes to Foggy Cityscapes, for example, we improve the detection accuracies by more than 11.90% in terms of mAP compared with the original model, i.e., DA-Faster. In our future work, we will expand cross-domain object detection to multiple different datasets to further improve the generalization ability.

Acknowledgments

We acknowledge support from the Youth Project of the Provincial Natural Science Foundation of Anhui 1908085QF285, the University Natural Sciences Research Project of Anhui Province KJ2020A0661, the National Natural Science Foundation of China under grant 61673359, the Key Research Plan of Anhui 202104d07020006, as well as the Hefei Specially Recruited Foreign Expert program.

References

- [1] T. Lin, M. Maire, S. J. Belongie, J. Hays, P. Perona, D. Ramanan, P. Dollár, C. L. Zitnick, Microsoft COCO: common objects in context, in: 13th European Conf. on Computer Vision (ECCV’14), Springer, 2014, pp. 740–755.
- [2] X. Dai, Y. Chen, B. Xiao, D. Chen, M. Liu, L. Yuan, L. Zhang, Dynamic head: Unifying object detection heads with attentions, in: IEEE Conf. on Computer Vision and Pattern Recognition (CVPR’21), 2021, pp. 7373–7382.
- [3] Y. Chen, W. Li, C. Sakaridis, D. Dai, L. Van Gool, Domain adaptive faster R-CNN for object detection in the wild, in: IEEE/CVF Conf. on Computer Vision and Pattern Recognition (CVPR’18), 2018, pp. 3339–3348.

- [4] J. Yosinski, J. Clune, Y. Bengio, H. Lipson, How transferable are features in deep neural networks?, in: *Advances in Neural Information Processing Systems 27: Annual Conf. on Neural Information Processing Systems 2014 (NIPS'14)*, 2014, pp. 3320–3328.
- [5] M. Cordts, M. Omran, S. Ramos, T. Rehfeld, M. Enzweiler, R. Benenson, U. Franke, S. Roth, B. Schiele, The cityscapes dataset for semantic urban scene understanding, in: *IEEE Conf. on Computer Vision and Pattern Recognition (CVPR'16)*, IEEE, 2016, pp. 3213–3223.
- [6] C. Sakaridis, D. Dai, L. Van Gool, Semantic foggy scene understanding with synthetic data, *Intl. Journal of Computer Vision* 126 (9) (2018) 973–992.
- [7] O. Tasar, Y. Tarabalka, A. Giros, P. Alliez, S. Clerc, StandardGAN: Multi-source domain adaptation for semantic segmentation of very high resolution satellite images by data standardization, in: *IEEE/CVF Conf. on Computer Vision and Pattern Recognition (CVPR'2020) Workshops*, IEEE, 2020, pp. 747–756.
- [8] W. Li, F. Li, Y. Luo, P. Wang, J. Sun, Deep domain adaptive object detection: A survey, in: *IEEE Symposium Series on Computational Intelligence (SSCI'20)*, IEEE, 2020, pp. 1808–1813.
- [9] Y. Chen, H. Wang, W. Li, C. Sakaridis, D. Dai, L. Van Gool, Scale-aware domain adaptive faster R-CNN, *Intl. Journal of Computer Vision* 129 (7) (2021) 2223–2243.
- [10] S. Ren, K. He, R. Girshick, J. Sun, Faster R-CNN: towards real-time object detection with region proposal networks, *IEEE Transactions on Pattern Analysis and Machine Intelligence* 39 (6) (2016) 1137–1149.
- [11] Z. Zhao, P. Zheng, S. Xu, X. Wu, Object detection with deep learning: A review, *IEEE Transactions on Neural Networks and Learning Systems* 30 (11) (2019) 3212–3232.

- [12] J. Redmon, A. Farhadi, YOLOv3: An incremental improvement, in: arXiv preprint, Vol. arXiv:1804.02767v1 [cs.CV] 8 Apr 2018, Cornell University Library, Ithaca, NY, USA, 2018.
- [13] G. J. et al., YOLOv5 (2021).
URL <https://github.com/ultralytics/yolov5>
- [14] W. Liu, D. Anguelov, D. Erhan, C. Szegedy, S. E. Reed, C. Fu, A. C. Berg, SSD: single shot multibox detector, in: 14th European Conf. on Computer Vision (ECCV'16), Springer, 2016, pp. 21–37.
- [15] M. Najibi, M. Rastegari, L. S. Davis, G-CNN: an iterative grid based object detector, in: IEEE Conf. on Computer Vision and Pattern Recognition (CVPR'16), IEEE, 2016, pp. 2369–2377.
- [16] C. Fu, W. Liu, A. Ranga, A. Tyagi, A. C. Berg, DSSD : Deconvolutional single shot detector, in: arXiv preprint arXiv:1701.06659v1 [cs.CV] 23 Jan 2017, Cornell University Library, Ithaca, NY, USA, 2017.
- [17] Z. Shen, Z. Liu, J. Li, Y. Jiang, Y. Chen, X. Xue, DSOD: learning deeply supervised object detectors from scratch, in: IEEE Intl. Conf. on Computer Vision (ICCV'17), IEEE, 2017, pp. 1937–1945.
- [18] R. B. Girshick, J. Donahue, T. Darrell, J. Malik, Rich feature hierarchies for accurate object detection and semantic segmentation, in: IEEE Conf. on Computer Vision and Pattern Recognition (CVPR'14), IEEE, 2014, pp. 580–587.
- [19] K. He, X. Zhang, S. Ren, J. Sun, Spatial pyramid pooling in deep convolutional networks for visual recognition, IEEE Transactions on Pattern Analysis and Machine Intelligence 37 (9) (2015) 1904–1916.
- [20] R. B. Girshick, Fast R-CNN, in: IEEE Intl. Conf. on Computer Vision (CVPR'15), IEEE, 2015, pp. 1440–1448.

- [21] J. Dai, Y. Li, K. He, J. Sun, R-FCN: object detection via region-based fully convolutional networks, in: *Advances in Neural Information Processing Systems 29: Annual Conf. on Neural Information Processing Systems*, 2016, pp. 379–387.
- [22] T. Lin, P. Dollár, R. B. Girshick, K. He, B. Hariharan, S. J. Belongie, Feature pyramid networks for object detection, in: *IEEE Conf. on Computer Vision and Pattern Recognition (CVPR’17)*, IEEE, 2017, pp. 936–944.
- [23] K. He, G. Gkioxari, P. Dollár, R. B. Girshick, Mask R-CNN, in: *IEEE Intl. Conf. on Computer Vision (ICCV’17)*, IEEE, 2017, pp. 2980–2988.
- [24] M. Khodabandeh, A. Vahdat, M. Ranjbar, W. G. Macready, A robust learning approach to domain adaptive object detection, in: *IEEE/CVF Intl. Conf. on Computer Vision (ICCV’19)*, IEEE, 2019, pp. 480–490.
- [25] Q. Cai, Y. Pan, C. Ngo, X. Tian, L. Duan, T. Yao, Exploring object relation in mean teacher for cross-domain detection, in: *IEEE Conf. on Computer Vision and Pattern Recognition (CVPR’19)*, IEEE, 2019, pp. 11457–11466.
- [26] A. Tarvainen, H. Valpola, Mean teachers are better role models: Weight-averaged consistency targets improve semi-supervised deep learning results, in: *Advances in Neural Information Processing Systems 30: Annual Conf. on Neural Information Processing Systems (NIPS’17)*, 2017, pp. 1195–1204.
- [27] J. Deng, W. Li, Y. Chen, L. Duan, Unbiased mean teacher for cross-domain object detection, in: *IEEE Conf. on Computer Vision and Pattern Recognition (CVPR’21)*, IEEE, 2021, pp. 4091–4101.
- [28] Z. He, L. Zhang, Domain adaptive object detection via asymmetric triway faster-rcnn, in: *16th European Conf. on Computer Vision (ECCV’20)*, Springer, 2020, pp. 309–324.
- [29] Q. Mou, L. Wei, C. Wang, D. Luo, S. He, J. Zhang, H. Xu, C. Luo, C. Gao, Unsupervised domain-adaptive scene-specific pedestrian detection for static video surveillance, *Pattern Recognition* 118 (2021) 108038.

- [30] L. Xiong, M. Ye, D. Zhang, Y. Gan, Y. Liu, Source data-free domain adaptation for a faster R-CNN, *Pattern Recognition* (2021) 108436.
- [31] A. Wu, Y. Han, L. Zhu, Y. Yang, Instance-invariant domain adaptive object detection via progressive disentanglement, *IEEE Transactions on Pattern Analysis and Machine Intelligence*.
- [32] R. Xie, F. Yu, J. Wang, Y. Wang, L. Zhang, Multi-level domain adaptive learning for cross-domain detection, in: *IEEE/CVF Intl. Conf. on Computer Vision Workshops, ICCV Workshops'19*, IEEE, 2019, pp. 3213–3219.
- [33] X. Zhu, J. Pang, C. Yang, J. Shi, D. Lin, Adapting object detectors via selective cross-domain alignment, in: *IEEE Conf. on Computer Vision and Pattern Recognition (CVPR'19)*, IEEE, 2019, pp. 687–696.
- [34] K. Saito, Y. Ushiku, T. Harada, K. Saenko, Strong-weak distribution alignment for adaptive object detection, in: *IEEE Conf. on Computer Vision and Pattern Recognition (CVPR'19)*, IEEE, 2019, pp. 6956–6965.
- [35] T. Kim, M. Jeong, S. Kim, S. Choi, C. Kim, Diversify and match: A domain adaptive representation learning paradigm for object detection, in: *IEEE Conf. on Computer Vision and Pattern Recognition (CVPR'19)*, IEEE, 2019, pp. 12456–12465.
- [36] W. Chen, H. Hu, Generative attention adversarial classification network for unsupervised domain adaptation, *Pattern Recognition* 107 (2020) 107440.
- [37] H. Wang, S. Liao, L. Shao, AFAN: augmented feature alignment network for cross-domain object detection, *IEEE Transactions on Image Processing* 30 (2021) 4046–4056.
- [38] C. Zhuang, X. Han, W. Huang, M. R. Scott, iFAN: image-instance full alignment networks for adaptive object detection, in: *The Thirty-Fourth AAAI Conf. on Artificial Intelligence (AAAI'20)*, AAAI, 2020, pp. 13122–13129.

- [39] C. Chen, Z. Zheng, X. Ding, Y. Huang, Q. Dou, Harmonizing transferability and discriminability for adapting object detectors, in: IEEE/CVF Conf. on Computer Vision and Pattern Recognition (CVPR’2020), IEEE, 2020, pp. 8866–8875.
- [40] Y. Liu, C. Ren, A two-way alignment approach for unsupervised multi-source domain adaptation, *Pattern Recognition* 124 (2022) 108430.
- [41] Y. Ganin, V. S. Lempitsky, Unsupervised domain adaptation by backpropagation, in: 32nd Intl. Conf. on Machine Learning (ICML’15), JMLR.org, 2015, pp. 1180–1189.
- [42] I. J. Goodfellow, J. Pouget-Abadie, M. Mirza, B. Xu, D. Warde-Farley, S. Ozair, A. C. Courville, Y. Bengio, Generative adversarial nets, in: Advances in Neural Information Processing Systems 27: Annual Conf. on Neural Information Processing Systems 2014 (NIPS’14), 2014, pp. 2672–2680.
- [43] A. Geiger, P. Lenz, C. Stiller, R. Urtasun, Vision meets robotics: The KITTI dataset, *The Intl. Journal of Robotics Research* 32 (11) (2013) 1231–1237.
- [44] M. Johnson-Roberson, C. Barto, R. Mehta, S. N. Sridhar, K. Rosaen, R. Vasudevan, Driving in the matrix: Can virtual worlds replace human-generated annotations for real world tasks?, in: IEEE Intl. Conf. on Robotics and Automation (ICRA’17), IEEE, 2017, pp. 746–753.
- [45] K. Simonyan, A. Zisserman, Very deep convolutional networks for large-scale image recognition, in: Conf. Track of the 3rd Intl. Conf. on Learning Representations (ICLR’15), 2014, pp. 1–14.
- [46] A. Krizhevsky, I. Sutskever, G. E. Hinton, ImageNet classification with deep convolutional neural networks, in: Advances in Neural Information Processing Systems 25: The 26th Annual Conf. on Neural Information Processing Systems (NIPS’12), 2012, pp. 1106–1114.